TEKNOKOM : Jurnal Teknologi dan Rekayasa Sistem Komputer
Vol. 5, No. 1, March 2022, pp. 78 - 87
ISSN: 2686-3219, DOI: 10.31943/teknokom. v5i1.68

ANALYSIS OF THE INFLUENCE OF LOOSE TERMINATION LEVEL WITH INCREASING TERMINATION TEMPERATURE OF ELECTRICAL EQUIPMENT USING INFRARED THERMOGRAPHY

Pranoto Budi Laksono[1*]
[1]Department of Electrical Engineering, Universitas Pamulang, Indonesia

ARTICLE INFO

History of the article:
Received September 1, 2021
Revised October 27, 2021
Accepted November 16, 2021
Published March 2, 2022

Keywords:
Temperature
Loose Termination
Infrared Thermography
Torque

ABSTRACT

The use of electrical energy in the industrial is very important to drive production machines. Machine maintenance is carried out so that the lifetime of the machine becomes longer so that the production process continues. Temperature is one of the most common indicators of the structural health of equipment and components. This means that the main symptoms of damage to machines and equipment can be indicated by increasing the temperature of the equipment. One of the symptoms of an increase in equipment temperature is due to a loose cable termination. The use of infrared thermography to measure the temperature rise due to loose termination is one of the methods in electrical machine maintenance. Previous studies using infrared thermography to measure the temperature rise due to loose termination have been carried out by many researchers, but these studies did not show a correlation between the level of loose termination and the increase in temperature but only stated that the loose termination caused an increase in temperature. This study focuses on finding the relationship between the level of loose termination compared to standard torque and the increase in temperature at the termination point. This is very useful as a quick overview in determining the level of urgency in maintenance activity, that percentage of loose termination of a certain value below the standard will give an increase in temperature of a certain value as well. This study resulted, for the torque setting condition 67% below the standard (loose) the temperature increase at the terminal was 13.4% - 15.6%, for the torque setting condition 33% below the standard temperature increase at the terminal of 12.3% -13.8% which mean that the increase in temperature is directly proportional to the level of slack termination and is also directly proportional to the increase in the motor speed. If the termination torque level is lower and the motor speed is increased, the terminal temperature rise will be drastically rise.

Correspondence:
Pranoto Budi Laksono
Department of Electrical Engineering,
Universitas Pamulang, Indonesia,
Email: dosen02629@unpam.ac.id

INTRODUCTION

A large organization in the engineering and insurance industry recently revealed that more than 30% of their total losses are caused by electrical and mechanical problems. Temperature is one of the most common indicators of the structural health of electrical equipment and components [1]. When analyzing electrical failures, it is revealed that about 20 to 25% of the total failures are the result of connection failures due to poor terminations and loose connections. In general, poor terminations / loose connections in the electrical system cause overheating of these connections which in turn leads to equipment failure [2]. This means that the main symptoms of damage to machinery and equipment can be indicated by the increase in temperature of the equipment.

The temperature that is used as an indicator of whether a machine is healthy or not is influenced by several factors. The increase in the temperature of the machine or equipment can be caused by misalignment of the pulley [3], damage to the bearing [4], poor connection/termination between cables, or between cables and switchgear or bus bars, incorrect selection or design of switchgear, line-overload , defects in cables and insulators or

faulty power meter connections [1], and can also be caused by other factors, for example during installation the termination is not tight compared to the standard torque.

D. Lopez-Perez et al [5] conducted a study using infrared thermography to analyze the temperature that arises significantly in induction motors, several times his research found, from the high-temperature several causes were found such as loose motor termination connections (unbalanced), loose belt settings, coil resistance unbalanced motor between phases. From this research, it is not stated that there is a relationship between the level of loose termination of the cable and the loosening of the setting belt which causes an increase in temperature.

M.W Hoffman et al [6] conducted research by integrating infrared sensors and machine learning for predictive maintenance of medium voltage switchgear. In electric current, the temperature rise can be due to damage, loose connection or corrosion, which causes an increase in electrical contact resistance, the presence of this temperature rise can be detected through temperature monitoring. This temperature increase is used as the basis for predicting switchgear maintenance. This study also did not mention the relationship of how loose the termination, nor the level of corrosion to changes in temperature.

The increase in temperature due to a loose termination without knowing the level value will make it difficult to determine the priority scale for engine maintenance due to the heavy engine maintenance load. This research is focused on investigating the correlation between the level of loose termination cable and the temperature rise at the termination point, as a reference in determining the level of urgency whether the increase in temperature must be controlled immediately or can be delayed for some time according to the priority scale. Section 2 will discuss the literature review which correlation with this research. Section 3, it is explained the research methodology carried out by the author to obtain data. Section 4 presents the data and analysis of the experimental results, and section 5 presents the conclusions from the results of this research.

RESEARCH METHOD

Infrared Thermography

Infrared Thermography is the science of detecting infrared energy emitted from an object, converting it to a pseudo temperature, and displaying the result as an infrared image. Literally, Infrared thermography (IRT) means “more-red” (infrared)” temperature image [1].

Infrared Thermography, or IR imaging, is a technique of non-contact recording and visualization of thermal radiation from objects, first of all, intended to analyze the distribution of surface temperatures. Electromagnetic radiation (thermal, or IR) occurs in solids, liquids, and gases due to the oscillations of atoms in the lattice or the oscillating motion of rotating molecules. Infrared radiation occupies the wide band of the electromagnetic spectrum from 0.75 μm (400 THz), or 750 nm to 1000 μm (300 GHz) or 1 mm, between visible light and radio waves [7]. For example

Kirchhoff's law reveals an important fundamental feature of media that provides the relationship between emissivity and absorbance. At any point on the surface of the 'heat emitter', at a given temperature and wavelength, the spectral emissivity is equal to the spectral absorbance for the oppositely directed non-polarizing radiation. In practice, this means that the absorbance (αλ) and emissivity (ελ) coefficients are the same numerically as Eq.1.

$$\alpha\lambda = \varepsilon\lambda \quad (1)$$

Kirchhoff's law can also be said that a good absorber is a good emitter. this statement can be interpreted as an absorbance/emission phenomenon and identify a more correct infrared thermometer reading [7].

Thermal radiation with a power density corresponding to the emitting material is emitted into a spatial angle of π steradian. According to Lambert's law, the infrared imager will only capture a small part of this radiation at an angle Ω, Eq.2.

$$J_{\Omega} = R.\Delta S\frac{\Omega}{\pi}Cos\ \phi \quad (2)$$

where ∆S is the area read by the IR imager in the instantaneous field of view,ϕ is the angle between the viewing direction (angle Ω) and the direction normal to the scanned surface. the magnitude of the values of ∆S and Ω is determined by the IR detector area and the lens parameters [7].

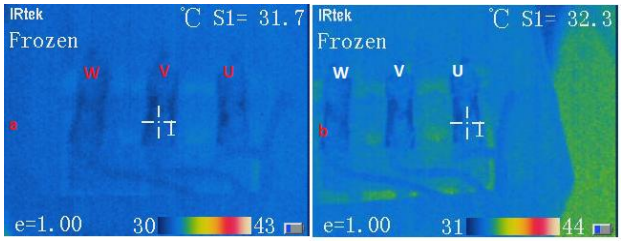

Figure 1. An example of using IR Thermography to measure motor induction terminals

Measurements using infrared thermography have several advantages, namely they do not interfere with the dielectric requirements of the equipment because they are non-contact, [8], [9], [10] the radiations are not detected by the human eye(save), [11], [12] non-destructive inspection technic [13], [14], [15] and free from electromagnetic interference due to placement in areas of low magnetic or electric fields. In addition, there is no need to turn off the energized system at the time of inspection[16], it can also cover a large area, unlike sensor point measurement. This drastically reduces the number of sensors required [6].

Loose Termination Cable

The flow of electric current through a conductor generates heat in a process called Joule heating. According to Joule's first law, both current (I) “Ampere” and resistance (R) “Ohm” affect the amount of heat generated (P) “Watt” [6], where is formulated as Eq.3.

$$P \propto I^2R \quad (3)$$

The number of failures that occur (e.g., breakdown, loose connection, or corrosion) will increase the electrical contact resistance, thereby increasing the temperature at that point at which the presence of the failure can be detected by temperature monitoring. In addition, an increase in the current value will also produce more heat, which can accelerate damage and reduce the lifetime of electrical equipment. Some of the causes of loose terminations are due to ambient vibrations, also due to the installation of bolts with torques that are not up to standard, for example after maintenance activities [6] can also be caused by the selection of bolts and rings that are not appropriate.

Every electrical equipment that uses cable terminations uses bolts, in the manual book the equipment is equipped with standard bolt tightness. So when the circuit is installed, how tight the bolt can be using a wrench / screwdriver that has the ability to adjust the torque. Fig.2 shows an example of standard bolt tightness on an MCB which can be seen on the nameplate.

Figure 2. Example of Standard Bolt Tightness on MCB 25 Ampere

From the example in Fig.2, if the M5 size bolt is used, the torque setting of the bolt is 2.3 - 2.8 N.m, while if the M8 size bolt is used, the torque setting is 5.5 - 7.5 N.m. If the use of a torque below the standard as shown in the Fig.2 will cause a temperature increase at the termination point as described in Eq.3

Literature Review

Lopez-Perez et al [5] conducted research using infrared thermography to analyze the temperature that arises significantly in induction motors, some of his studies found that from these high temperatures several cases were found such as loose motor termination connections (not balanced), belt settings loose, unbalanced motor winding resistance between phases. From these cases, after completion of repairs according to the cause, then the temperature was re-measured and it turned out to have decreased significantly to normal conditions.

Glowacz et al [17] also conducted research on a 3-phase induction motor using infrared thermal imaging to diagnose the condition of the motor while operating. Glowacz experimented with three conditions, namely a normal motor, the second condition was a three-phase induction motor with damage to 2 bars (cage rotor), while the third used a 3-phase induction motor with damage to the cage rotor ring. The results of this data collection are classified and then analyzed using the MATLABS algorithm to produce recommendations for the motor conditions that are analyzed.

Resendiz-Ochoa et al [13] make a fault analysis research automatically using data from infrared thermography on induction motors with the focus of research on the condition of Broken Rotor Bar, Ball Bearing defect and Misalignment of the motor coupling to the gearbox. The results of infrared thermography measurements are validated using an RTD (Resistance

Temperature Detector) sensor. This data is entered into the database by a C++ software program to determine the severity of the fault being analyzed.

Roque A. et al [1] conveyed in his review journal about the use of infrared thermography in the industrial world to be used in analyzing root causes, especially for machines which are grouped into three categories: classification, namely electrical, mechanical and the last group mentioned "other". He recommends the use of infrared thermography for temperature analysis of machines because it can reduce machine maintenance costs compared to the classical method.

Morales-Perez et al [3] conducted a study using Infrared Thermography to analyze bearing conditions in three-phase induction motors. He also made three conditions, namely normal bearings, damaged bearing caps and finally using damaged bearings on the outer part. The three-phase motor was run with two conditions, namely with a frequency of 40 Hz and 60 Hz to determine the difference in temperature differences between the motors during the research process.

For a summary of the literature review from several researchers who have proposed and used by the author, see Table 1.

Table 1. Literature Review

Year	2017	2017	2018	2019	2019
Researcher	Lopez-Perez et al [5]	Glowacz et al [17]	Resendiz-Ochoa et al [13]	Roque A. Osornio-Rios, et al. [1]	Morales-Perez et al [3]
Methods	Infrared Thermography	Infrared Thermography and MATLAB	Infrared Thermography, C++, and use the RTD sensor	Infrared Thermography	Infrared Thermography
Object	Induction motor	Induction motor	Induction motor	Industrial machines	Induction motor
Result	Loose termination, loose van belt, unbalanced windings resistance	Two motor cage broken, and motor ring broken	The rotor bar is broken, the ball bearing is broken, and a couple of misalignment	Recommend using infrared thermography with the aim of cost reduction on maintenance costs compared to the classical method.	broken bearing cover, damaged outer bearing

Research Methodology

The electrical circuit design for this research can be grouped into 3 main parts, namely the power, control and load sections, as shown in the block diagram in Fig.3.

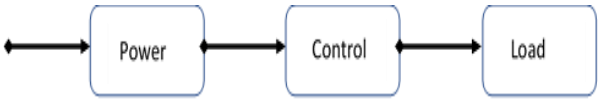

Figure 3. Block Diagram

The power section consists of the MCB as a breaker and connector for the power source, the control section consists of the "Mitsubishi" Variable Speed Drive as a regulator of the rotational speed of the induction motor. The inverter parameters set by the researcher include acceleration, deceleration, input commands and others which are summarized in detail in Table 2.

Table 2. VSD Parameter Setting

VSD Parameter	Setting
Acceleration Time	10 second
Deceleration Time	10 second
Maximum Frequency	50Hz
Frequency Reference	20Hz, 40Hz, 50Hz
Input Command	Key-Pad

For the load section in the form of a 3 phase induction motor 5.5 KW, 11.1 Ampere, 380 V, 1450 rpm and for standard torque (τ) the tightness of the U, V, W terminals is 1.5 Nm as shown in Fig.4. The measuring instrument used is the IR thermograph type Ti50 series, Irtek brand. Terminal torque setting using a torque screwdriver "Toptul" which can be set the torque value (Fig.5).

Figure 4. Induction Motor 5,5 KW

Figure 5. IR Thermograph and Variable Torque Wrench

The testing methodology is that the motor is connected to a VSD (Variable Speed Drive) where terminals V and W are set to a torque of 1.5 Nm (according to standard) while terminal U is set to 3 conditions, namely τ_1= 0,5 Nm (67% below standard), τ_2 = 1 Nm (33% below standard), and τ_3 = 1,5 Nm (same with standard). Each different torque setting condition was tested with 3 different motor speeds, namely 20Hz, 40Hz, and 50Hz. For each setting condition, the temperature data is taken starting at 0 hour, 2nd hour, 4th hour, 6th hour and finally 8th hour.

Terminal temperature data retrieval is carried out with an IR thermography and validated using a multi-tester with a thermocouple base.

RESULTS AND DISCUSSION

The complete of measurement data is shown in the following Table 3 until Table 9. τ_1 is 1st torque setting, TU-20U,TU-40U, TU-50U represents the temperature value measured by the multi-tester at terminal U when the speed setting conditions are 20Hz, 40Hz, and 50Hz. If denoted V means the measurement at the terminal V. IR-20U, IR-40U, IR-50U is represents the temperature value measured by the Infrared Thermography at terminal U when the speed setting conditions are 20Hz, 40Hz, and 50Hz too.

From Table 3 to Table 5 and the graphs in Fig.6 and Fig.7 (left) can be explained as follows, when terminal U is set to a torque of 0.5 Nm and terminal V, W is set to a torque of 1.5 Nm and the motor is tested to rotate with a frequency of 20 Hz, at 0 o'clock (about 10 minutes from the moment it is turned on) the temperature of terminal U (IR-20U) is 30.1 ^oC while the temperature of terminal V (IR-20V) is 30.3 ^oC, meaning that the initial temperature of each terminals like that. When the motor has been running for about 2 hours, a second measurement is made, the IR-20U is 31.2^oC and the IR-20V is 30.5 ^oC, and so on until the 8th hour (meaning 8 hours from the start of operation). It can be seen that the temperature increase at terminal U tends to be higher (temperature increase of 13.6%) compared to terminal V (11.6%) during the 8-hour test process. The graph is shown with a red line for terminal U and a black line for terminal V. For the blue and brown bar graphs are comparative data taken using another temperature measuring instrument (multitester with thermocouple sensor). It can be seen that the trend is similar to the results of measurements using an infrared thermograph. The same thing is also seen for the frequency settings of 40Hz (15.6% compared to 11.6%) and 50 Hz (13.4% compared to 7%) with a torque treatment of 0.5 Nm at terminal U, and 1.5 Nm to terminal V and W. These measurement conditions done with a torque setting of 67% below standard.

Table 3 . Temperature data at τ_1=0,5 Nm and τ_3 1,5 Nm and speed 20Hz

Torque Setting (τ)	Terminal U-- τ_1 = 0,5 Nm Terminal V-- τ_3 =1,5 Nm			
Freq.Sett.	20 Hz			
Time (hours)	TU-20U (^oC)	TU-20V (^oC)	IR-20U (^oC)	IR-20V (^oC)
0	31,2	30,5	30,1	30,3
2	30,6	30,4	31,2	30,5
4	32,4	32,2	34,2	33,8
6	31,9	31,6	32,3	32,3
8	31,3	30,7	32,3	31,5
Min	30,6	30,4	30,1	30,3
Max	32,4	32,2	34,2	33,8
Max-Min	1,8	1,8	4,1	3,5
Average	31,48	31,08	32,02	31,68
% temp. Increase	5,9%	5,9%	13,6%	11,6%
Difference			2%	
% Torque	67%	Obtained from ((1,5Nm-0,5Nm)/1,5Nm) x 100%		

Table 4. Temperature data at τ_1 0,5 Nm and τ_3 1,5 Nm and speed 40Hz

Torque Setting (τ)	Terminal U -- τ_1 = 0,5 Nm Terminal V-- τ_3 = 1,5 Nm			
Freq.Sett.	40 Hz			
Time (hours)	TU-40U (ºC)	TU-40V (ºC)	IR-40U (ºC)	IR-40V (ºC)
0	29,2	29,1	30,1	30,3
2	31,1	31,1	32,9	32,7
4	31,3	31,1	34	33,8
6	31,5	31,3	33,2	32,3
8	31,7	31,4	34,8	30,9
Min	29,2	29,1	30,1	30,3
Max	31,7	31,4	34,8	33,8
Max-Min	2,5	2,3	4,7	3,5
Average	30,96	30,8	33	32
% temp. Increase	8,6%	7,9%	15,6%	11,6%
Difference			4%	
% Torque	67%	Obtained from ((1,5Nm-0,5Nm)/1,5Nm)x 100%		

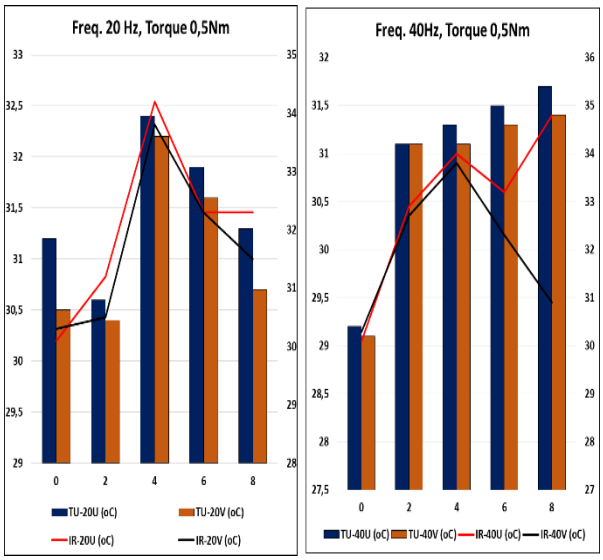

Figure 6. Graph of Temperature Measurement Data for terminals U (τ_1 = 0.5 Nm) and V(τ_3 = 1.5 Nm) with frequency setting 20Hz (left) and 40Hz (right)

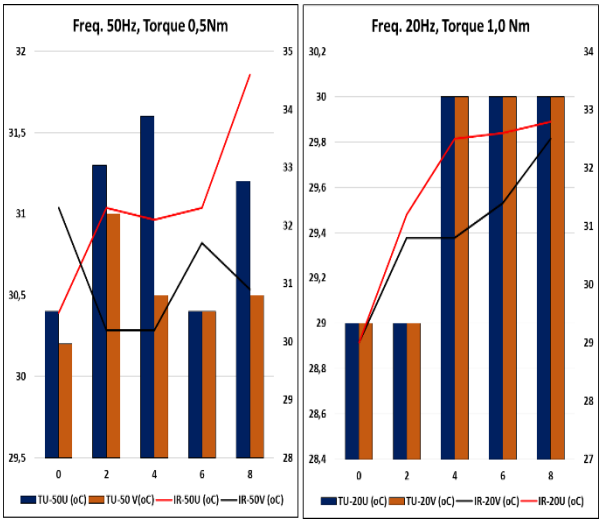

Figure 7. Graph of Temperature Measurement Data for *(left)* → terminals U (τ_1 = 0.5Nm) and V(τ_3 = 1.5 Nm) with frequency setting 50Hz, *(right)* → τ_1 = 1 Nm and 40Hz

Table 5. Temperature data at τ_1=0,5 Nm and τ_3 1,5 Nm and speed 50Hz

Torque Setting (τ)	Terminal U-- τ_1 = 0,5 Nm Terminal V-- τ_3 = 1,5 Nm			
Freq.Sett.	50 Hz			
Time (hours)	TU-50U (ºC)	TU-50 V(ºC)	IR-50U (ºC)	IR-50V (ºC)
0	30,4	30,2	30,5	32,3
2	31,3	31	32,3	30,2
4	31,6	30,5	32,1	30,2
6	30,4	30,4	32,3	31,7
8	31,2	30,5	34,6	30,9
Min	30,4	30,2	30,5	30,2
Max	31,6	31	34,6	32,3
Max-Min	1,2	0,8	4,1	2,1
Average	30,98	30,52	32,36	31,06
% temp. Increase	3,9%	2,6%	13,4%	7,0%
Difference			6,6%	
% Torque	67%	Obtained from ((1,5Nm-0,5Nm)/1,5Nm)x 100%		

Table 6. Temperature data at τ_3 =1 Nm and τ_3 =1,5 Nm and speed 20Hz

Torque Setting (τ)	Terminal U —τ_1 = 1 Nm Terminal V-- τ_3 =1,5 Nm			
Freq.Sett.	20 Hz			
Time (hours)	TU-20U (°C)	TU-20V (°C)	IR-20U (°C)	IR-20V (°C)
0	29	29	29	29
2	29	29	31,2	30,8
4	30	30	32,5	30,8
6	30	30	32,6	31,4
8	30	30	32,8	32,5
Min	29	29	29	29
Max	30	30	32,8	32,5
Max-Min	1	1	3,8	3,5
Average	29,6	29,6	31,62	30,9
% temp. Increase	3,4%	3,4%	13,1%	12,1%
Difference			1%	
% Torque	33%	Obtained from ((1,5Nm-1Nm)/1,5Nm)x 100%		

Table 7. Temperature data at τ_1=1 Nm and τ_3=1,5 Nm and speed 40Hz

Torque Setting (τ)	Terminal U-- τ_1 = 1 Nm Terminal V-- τ_1 = 1,5 Nm			
Freq.Sett.	40 Hz			
Time (hours)	TU-40U (°C)	TU-40V (°C)	IR-40U (°C)	IR-40V (°C)
0	30,1	29,8	28,9	28,4
2	31,6	31,4	29,8	29,1
4	31,3	31,3	32,9	31,9
6	30,8	30,5		
8	32,5	32,2		
Min	30,1	29,8	28,9	28,4
Max	32,5	32,2	32,9	31,9
Max-Min	2,4	2,4	4	3,5
Average	31,26	31,04	30,53	29,8
% temp. Increase	8,0%	8,1%	13,8%	12,3%
Difference			1,3%	
% Torque	33%	Obtained from ((1,5Nm-1Nm)/1,5Nm)x 100%		

Tables 6 to Table 8 and the graphs in Fig.7 (right) and Fig.8 present measurement data with the condition for the U terminal the bolt torque is set to 1 Nm or 33% below the standard value, while the V and W terminals are still the same, namely 1.5 Nm (100% according to standard torque). The frequency setting treatment is still the same, namely three conditions, 20Hz, 40Hz, and 50Hz. The trend condition is similar to the trend in the previous graph in Fig.6 and Fig.7 (left), namely terminals U and V during the testing process experienced an increase in temperature, but for terminal U tended to be higher than terminal V (13.1% compared to 12.1%, 13.8% compared to 12.3% and 12.3% compared to 7.8%). For data that is empty in the 40 Hz frequency column, namely at 6 and 8 hours, this is because there are technical problems where the infrared thermograph battery is low and needs to be recharged for a long time, so no data is measured with the infrared thermograph. For conditions, each frequency setting shows a trend similar to the previous data.

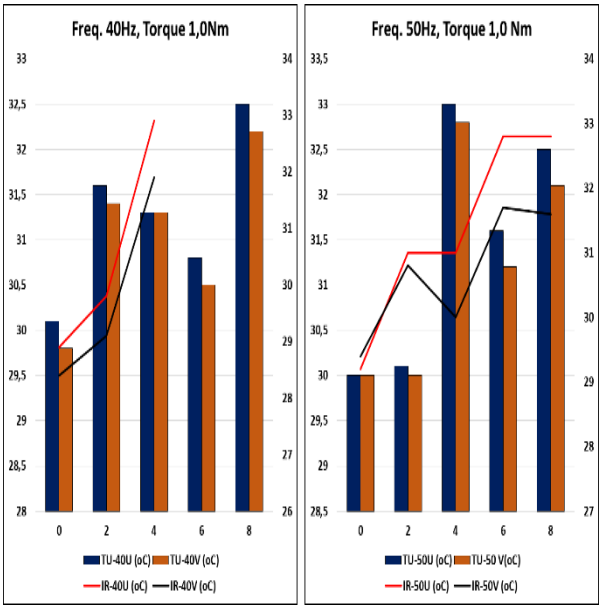

Figure 8. Graph of Temperature Measurement Data for terminals U (τ_1 = 1 Nm) and V(τ_3 = 1.5 Nm) with frequency setting 40Hz (left) and 50Hz (right)

Table 8. Temperature data at τ_1 =1 Nm and τ_3 =1,5 Nm and speed 50Hz

Torque Setting (τ)	Terminal U—τ_1 =1 Nm Terminal V-- τ_3 =1,5 Nm			
Freq.Sett.	50 Hz			
Time (hours)	TU-50U (ºC)	TU-50 V(ºC)	IR-50U (ºC)	IR-50V (ºC)
0	30	30	29,2	29,4
2	30,1	30	31	30,8
4	33	32,8	31	30
6	31,6	31,2	32,8	31,7
8	32,5	32,1	32,8	31,6
Min	30	30	29,2	29,4
Max	33	32,8	32,8	31,7
Max-Min	3	2,8	3,6	2,3
Average	31,44	31,22	31,36	30,7
% temp. Increase	10,0%	9,3%	12,3%	7,8%
Difference			4,5%	
% Torque	33%	Obtained from ((1,5Nm-1Nm)/1,5Nm)x 100%		

Table 9 and the graph in Fig.9 present measurement data for the standard condition of the motor terminal torque of 1.5 Nm. It looks similar to the data in Tables 3 to 5 and Tables 6 to Table 8 that the increase in the duration of operating hours causes an increase in terminal temperature. However, when viewed from the trend from 0 to 8 hours, the temperature increase is almost similar between terminal U and terminal V, although there is still a small difference in value between the two, which is about 8.6% compared to 9.7%

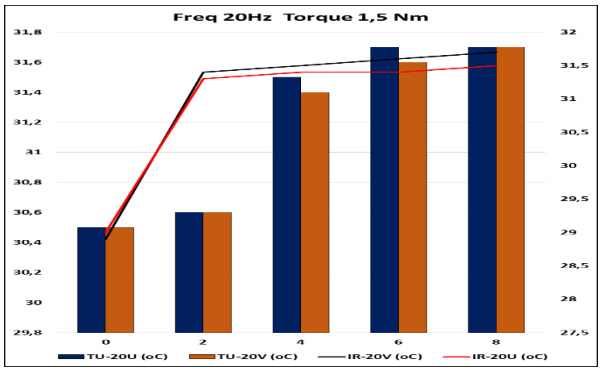

Figure 9. Graph of Temperature Measurement Data for terminals U=V (τ_1= τ_3 = 1,5Nm) with frequency setting 20Hz

Table 9. Temperature data at τ_1= τ_3 =1,5 Nm and speed 20 Hz

Torque Setting (τ)	Terminal U,V,W-- τ_3 =1,5 Nm			
Freq. Sett.	20 Hz			
Time (hours)	TU-20U (ºC)	TU-20V (ºC)	IR-20U (ºC)	IR-20V (ºC)
0	30,5	30,5	29	28,9
2	30,6	30,6	31,3	31,4
4	31,5	31,4	31,4	31,5
6	31,7	31,6	31,4	31,6
8	31,7	31,7	31,5	31,7
Min	30,5	30,5	29	28,9
Max	31,7	31,7	31,5	31,7
Max-Min	1,2	1,2	2,5	2,8
Average	31,2	31,16	30,92	31,02
% temp. Increase	3,9%	3,9%	8,6%	9,7%
Difference			-1,1%	
% Torque	0%	Torque Set = standard		

Based on the formula in Eq.3, where the electric power is proportional to the square of the current multiplied by the resistance, it is also explained that according to Joule's law where heat can be affected by the value of current and resistance and for resistance it can be caused by either rust or a loose connection. This can be seen from the measurement data in Table 3 until Table 9 which show that the increasing of the temperature value to terminal U is greater than the increasing of temperature to terminal V. These data indicate that terminal U is set with a lower bolt tightness torque than the standard causing an increase in the value of the resistance at the terminal cable and causes an increase in the value of the current flowing. The magnitude of the temperature increase in this experiment is not so large. For setting torque of 67% below standard it gives an increase in terminal temperature of 13.4% - 15.6%, while for setting torque of 33% below standard it gives a temperature increase of 12.3% -13.8%, this is due to the current flowing too small (average 0.95A) compared to the current stated on the motor nameplate (11.1A) or only about 8.56%.

This small electric current is caused by a no-load motor. If the motor is added to a load that can be adjusted to a large or small value, so that it can produce an electric current close to the current value on the nameplate, it shows the results of a significant difference in the temperature of the U and V terminals.

Based on the data in Table 3 to Table 8, where the focus is on the "difference" column where this data is obtained from the difference between the percentage increase in temperature of terminal U and terminal V when compared to the increase in the motor frequency setting (motor speed). If summarized in one table it will look like in Table 10 and graph in the Fig.10.

Table 10. Difference Temperature Rise Vs Motor Speed

	20Hz	40Hz	50Hz
Difference (0,5 Nm)	2%	4%	6,60%
Difference (1,0 Nm)	1%	1,30%	4,50%

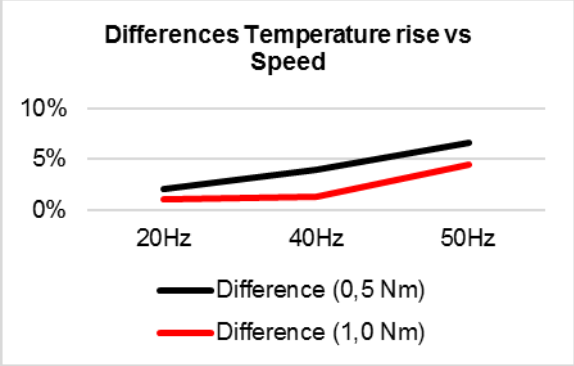

Figure 10. Differences Temperature rise vs Speed

Table 10 and the graph in Fig.10 shows that the increase in temperature is directly proportional to the level of slack termination is also directly proportional to the increase in motor speed. If the termination torque level is lower and the motor speed is increasing, the terminal temperature rise will be drastically higher.

CONCLUSION

The relationship between the level of loose termination and the temperature rise of the cable (at the termination point) is that the temperature at the termination point increase is directly proportional to the level of loose termination and also directly proportional to the increase in motor speed. If the termination torque level is lower and the motor speed is increased, the terminal temperature rise will drastically rise.

REFERENCES

[1] J. A. Roque A. Osornio-Rios, RJose A. Antonino-Daviu and R. De Jesus Romero-Troncoso, “Recent industrial applications of infrared thermography: A review,” *IEEE Trans. Ind. Informatics*, vol. 15, no. 2, pp. 615–625, 2019, doi: 10.1109/TII.2018.2884738.

[2] P. K. Gore and P. Gore, “Failure due to poor termination & loose connections in electrical systems,” *Water Energy Int.*, vol. 61RNI, no. 1, pp. 48–51, 2018.

[3] C. Morales-Perez, J. Rangel-Magdaleno, H. Peregrina-Barreto, J. Ramirez-Cortes, and E. Vazquez-Pacheco, “Bearing fault detection technique by using thermal images: A case of study,” *I2MTC 2019 - 2019 IEEE Int. Instrum. Meas. Technol. Conf. Proc.*, vol. 2019-May, pp. 1–6, 2019, doi: 10.1109/I2MTC.2019.8826953.

[4] A. Gugaliya, G. Singh, and V. N. A. Naikan, “Effective combination of motor fault diagnosis techniques,” *Proc. 2018 IEEE Int. Conf. Power, Instrumentation, Control Comput. PICC 2018*, pp. 1–5, 2018, doi: 10.1109/PICC.2018.8384812.

[5] D. Lopez-Perez and J. Antonino-Daviu, “Application of Infrared Thermography to Failure Detection in Industrial Induction Motors: Case Stories,” *IEEE Trans. Ind. Appl.*, vol. 53, no. 3, pp. 1901–1908, 2017, doi: 10.1109/TIA.2017.2655008.

[6] M. W. Hoffmann *et al.*, “Integration of novel sensors and machine learning for predictive maintenance in medium voltage switchgear to enable the energy and mobility revolutions,” *Sensors (Switzerland)*, vol. 20, no. 7, pp. 1–24, 2020, doi: 10.3390/s20072099.

[7] V. Vavilov and D. Burleigh, *Infrared Thermography and Thermal Nondestructive Testing*. Cham, Switzerland: Springer, 2020.

[8] S. Doshvarpassand, C. Wu, and X. Wang, “An overview of corrosion defect characterization using active infrared thermography,” *Infrared Phys. Technol.*, vol. 96, pp. 366–389, 2019, doi: https://doi.org/10.1016/j.infrared.2018.12.006.

[9] A. Ghahramani, G. Castro, S. A. Karvigh, and B. Becerik-Gerber, “Towards unsupervised learning of thermal comfort using infrared thermography,” *Appl.*

Energy, vol. 211, pp. 41–49, 2018, doi: https://doi.org/10.1016/j.apenergy.2017.11.021.

[10] A. Choudhary, D. Goyal, and S. S. Letha, "Infrared Thermography-Based Fault Diagnosis of Induction Motor Bearings Using Machine Learning," *IEEE Sens. J.*, vol. 21, no. 2, pp. 1727–1734, 2021, doi: 10.1109/JSEN.2020.3015868.

[11] A. W. Kandeal *et al.*, "Infrared thermography-based condition monitoring of solar photovoltaic systems: A mini review of recent advances," *Sol. Energy*, vol. 223, pp. 33–43, 2021, doi: https://doi.org/10.1016/j.solener.2021.05.032.

[12] M. Ortega, E. Ivorra, A. Juan, P. Venegas, J. Martínez, and M. Alcañiz, "MANTRA: An Effective System Based on Augmented Reality and Infrared Thermography for Industrial Maintenance," *Appl. Sci.*, vol. 11, no. 1, 2021, doi: 10.3390/app11010385.

[13] E. Resendiz-Ochoa, R. A. Osornio-Rios, J. P. Benitez-Rangel, R. D. J. Romero-Troncoso, and L. A. Morales-Hernandez, "Induction Motor Failure Analysis: An Automatic Methodology Based on Infrared Imaging," *IEEE Access*, vol. 6, no. c, pp. 76993–77003, 2018, doi: 10.1109/ACCESS.2018.2883988.

[14] F. Ciampa, P. Mahmoodi, F. Pinto, and M. Meo, "Recent advances in active infrared thermography for non-destructive testing of aerospace components," *Sensors (Switzerland)*, vol. 18, no. 2, 2018, doi: 10.3390/s18020609.

[15] Q. Fang, B. D. Nguyen, C. I. Castanedo, Y. Duan, and X. M. II, "Automatic defect detection in infrared thermography by deep learning algorithm," in *Thermosense: Thermal Infrared Applications XLII*, 2020, vol. 11409, pp. 180–195, [Online]. Available: https://doi.org/10.1117/12.2555553.

[16] A. Kirsten Vidal de Oliveira, M. Aghaei, and R. Rüther, "Aerial infrared thermography for low-cost and fast fault detection in utility-scale PV power plants," *Sol. Energy*, vol. 211, pp. 712–724, 2020, doi: https://doi.org/10.1016/j.solener.2020.09.066.

[17] A. Glowacz and Z. Glowacz, "Diagnosis of the three-phase induction motor using thermal imaging," *Infrared Phys. Technol.*, vol. 81, no. 11, pp. 7–16, 2017, doi: 10.1016/j.infrared.2016.12.003.